Chalcogenide Letters Vol. 14, No. 12, December 2017, p. 521 - 527

THERMAL BEHAVIOUR OF CdSe HOLLOW QDs STUDIED BY MOLECULAR DYNAMICS SIMULATIONS

S. SENTURK DALGIC*
Department of Physics, Trakya University, 22030 Edirne-Turkey

Thermally behavior of the different sizes of CdSe hollow quantum dots (HQDs) sub<10nm was first investigated by molecular dynamics (MD) simulations. The seven samples of the CdSe-HQDs within the thin wall thickness have constructed from the solid QDs with zincblende (ZB) structure at the diameter of 4-8m sizes. The size and temperature dependent cohesive energies, self-diffusion kinetics and the transformations in their morphology, thus their melting points have presented by describing the two-stage melting of HQDs. Although, the thermodynamic stability of the simulated HQDs is related to the hollow interior they contain, it is actually more concerned with their wall thickness. A two-step melting behavior is not observed for the HQDs with the diameter smaller than 5nm. However, it is identified clearly for 6nm size HQDs with two different melting modes by analyzing the self-diffusion behavior of atoms. Thus, these results can be suitable for the construction of chalcogenide HQDs with ZB structure

(Received November 17, 2017; Accepted December 6, 2017)

Keywords: Hollow Quantum Dots, CdSe, Thermal Effect, Cohesive Energy

1. Introduction

The chalcogenide semiconductor nanocrystals have attracted much attention due to their size-dependent physical properties and promising applications in nanoscience and nanotechnology. Chalcogenide based Quantum dots (ChQDs) are a special class of chalcogenide based nanomaterials, with crystals composed of only a few hundred to thousands of atoms due to their small size, around 2-10nm [1-3]. Among the ChQDs, CdSe QDs are preferred as model systems to study quantum size effects occurred at the nanoscale [3-9]. This effect quantizes the energy levels within the quantum dot with energy values directly related to quantum dot size [10]. The Cd chalcogenide QDs, exist in two different crystalline structure forms as cubic zincblende (ZB) and wurtzite (WZ) which atoms are placed in different stacking sequence with tetrahedrally coordinated. Based on the quantum size effect, ZB-CdSe QDs becomes a bright, highly stable, fluorescence nanoparticle because of higher PL efficiency than the WZ-CdSe QDs [4].

For this reason, CdSe QDs based semiconductor/metal nanocomposites are some new generation materials that the photo stability of CdSe QDs composites is well established and used for in-vitro and optical imaging, surface plasmon resonances applications, [5-8].

On the other hand, some experimental groups have obtained new generation CdSe nanostructures which are an alternative to zero dimension (0D) nanocrystals such as QDs [11] or different structured QDs [12].

Recently, the synthesized hollow CdSe NPs which can be utilized optoelectronic devices have been reported [12,13]. The CdSe hollow spheres were also obtained by different experimental formation processes [14] and also used as composite structures [8]. From a theoretical point of view, some first principle calculations and MD simulations for the bulk structural properties of CdSe were established by a variety of methods [14,15]. The high-quality thermal behavior of ZB-CdSe nanoparticles have been successfully obtained [16], but much less attention has been paid on

*Corresponding author: serapd@trakya.edu.tr

ZB-CdSe based HQDs (<10nm), and there is still lacking systematic studies on ZB-CdSe HQDs as comparative researches relative to usual solid CdSe-QDs. The thermodynamic properties and melting behaviors of hollow structure QDs are still not well known which is important for their nano technologic applications. Hollow structures are difficult to understand some features from experiments due to the nanoscale. Thus, computational methods, such as MD simulations are powerful tool for that investigations

In this work, the thermal effects of hollow interior and wall thicknesses on the thermodynamic stability of CdSe HQDs sub <10nm was investigated. Here, for the first time, the thermal behavior of CdSe-HQDs with different sizes has studied by MD simulations. According to our knowledge, no detailed investigation of the temperature and size-dependent phase transformations of ZB-CdSe HQDs has been performed by molecular dynamics until now. In attempting to explain the thermal behavior of CdSe-HQDs, the empirical three body interatomic potential of Tersoff has been used [17,18] by DLPOLY-simulation code [19].

2. Materials and method

MD simulations may determine the physical properties of nanomaterials at the atomic level. Here, it has been performed with CdSe-QDs with hollow interior.

2.1. Materials and Model Construction

The simulated CdSe-HQDs were constructed through a top-down method as follows: First, a large cube of CdSe was built in the cubic ZB -diamond structure. A solid sphere represented as a quantum dot was extracted from the ZB-CdSe crystal cube of 216000 atoms with the lattice parameter, 0.6055nm, by cutting in the [111] crystallographic direction using a series of spherical cutoff centered at a core of cube. Then, removing atoms from the center of the nanoparticle leaves a cavity space inside and thus forms a hollow nanoparticle. The hollow system has attributed to an inner-outer radius, r, and R, respectively, while t is the wall thickness as (R-r). The seven different sizes of CdSe HQDs are formed as one-layer shell contains two elements, Cd (cadmium) and Se (selenium) with an atomic ratio of 1:1, respectively. The number of particles studied here is given in Table 1.

Table 1. Size of the CdSe-HQDs used for investigation

Solid CdSe QDs	CdSe-HQDs			
Radii of QDs	Number of atoms t=1nm	Number of atoms t=1.5nm	Number of atoms t=2nm	Number of atoms t=2.5nm
2nm	1048	1190	-	-
3nm	2902	3620	3950	-
4nm	-	-	8474	9192

2.2. Method

The many body potentials for the interatomic interactions in our MD simulations are modeled with a three-body Tersoff potential (TP) based on the bond-order concept with the strength of a bond between two atoms depends on the local atomic environment [17, 18]. The interatomic potential energy between i and j atoms is given by

$$V_{ij} = f_c(r_{ij})[Aa_{ij}\exp(-\lambda_1 r_{ij}) - Bb_{ij}\exp(-\lambda_2 r_{ij})] \quad (1)$$

$$f_c(r_{ij}) = \begin{cases} 1, r < R - D \\ \frac{1}{2} - \frac{1}{2}\sin\left[\frac{\pi}{2}\frac{(r-R)}{D}\right], R - D < r < R + D \\ 0, \mathrm{r} > \mathrm{R} + \mathrm{D} \end{cases} \quad (2)$$

where a_{ij} and b_{ij} terms are the bond order parameters for the repulsive and attractive part of the potential energy, V_{ij} respectively. These parameters describe how the bond-order formation energy affected by the presence of other neighboring atoms such as the positions of k atoms. They have formed

$$a_{ij} = (1+\alpha^n \eta_{ij}^n)^{-1/(2n)} \qquad b_{ij} = (1+\beta^n \xi_{ij}^n)^{-1/(2n)} \tag{3}$$

with

$$\xi_{ij} = \sum_{k \neq i,j} f_c(r_{ij}) g(\theta_{ijk}) \exp[\lambda_3^3 (r_{ij} - r_{ik})^3] \tag{4}$$

$$\eta_{ij} = \sum_{k \neq i,j} f_c(r_{ij}) g(\theta_{ijk}) \exp[\lambda_3^3 (r_{ij} - r_{ik})^3] \tag{5}$$

$$g(\theta) = 1 + \frac{c^2}{d^2} - \frac{c^2}{d^2 + (h - \cos\theta)^2} \tag{6}$$

Where ξ and η are the effective coordination numbers and $g(\theta)$ is a function of the angle between r_{ij} and r_{ik}. The potential parameters A, B, λ_1, λ_2, n, β, h, c and d were determined for the ZB phase of CdSe using the bulk heat of formation by Benkabou and co-workers [18]. These parameters have produced the bulk lattice parameter for CdSe within %0.08 and used for potential applications of nanoplates [20] and nanoparticles [21] by MD simulations.

2.3. Simulations Procedure

MD simulations were carried out for both CdSe-QDs and CdSe-HQDs in ZB structure using TP force field together with long ranged Coulomb forces. The classic simulations have been performed using the DL_POLY classic version 2.18 package [19].

All MD simulations were performed in Isochoric-Isothermal (NVT) ensemble under heating. The equations of atomic motions with a time step as 1fs have integrated by the leapfrog Verlet Velocity algorithm. Brendsden thermostat controlled the temperature of the system with 0.5 value in all simulations. The optimization procedure has applied to obtain the equilibrium structures at 0K. First, the initial samples annealed fully at 25K, followed by a cooling process with the temperature interval of 5K. Then the optimized HQDs were heated up to 1600K with an increment of 25K. On the other hand, the computational details for bulk ZB-CdSe simulation procedure can be found elsewhere [18, 21].

3. Results and discussion

In this study, the thermodynamic stability of CdSe-HQDs at different temperatures have investigated through the changes in morphology and the thermodynamic properties during the heating process, such as snapshots of atomic arrangements at different temperatures, caloric curves, heat capacity and self-diffusion coefficients. The cohesive energies per atom were calculated at different temperatures for the CdSe-HQDs with different radius. The calculated cohesive energies for the HQDs containing N=1048 and N=1190 atoms with 1-1.5nm wall thickness are presented in Fig.1.

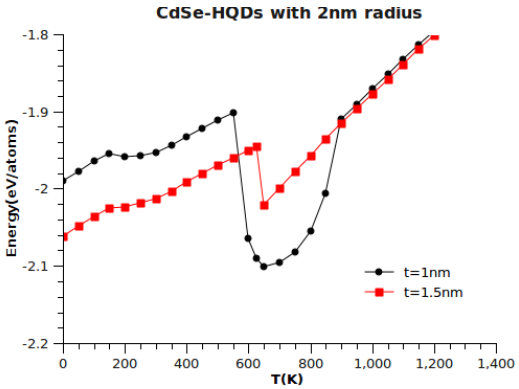

Fig.1. Temperature dependence of the cohesive energy of CdSe-HQDs with 4nm size

As can be seen from Fig. 1, the cohesive energy curve shows a sharp decrease for the wall thickness of 1nm case rather than 1.5nm which corresponds to the melting temperature of the inner shell of the hollow interior. However, it starts to melt earlier as before 550K in comparison with 600K that obtained for the 1.5nm wall thickness.

The snapshots of cross sections front view and sliced in [010] direction of the HQDs for the atomic arrangement of the 2nm radius with N1190 atoms are illustrated in Fig.2a and Fig.2b, respectively. OVITO package is used to demonstrate these atomic arrangements [22].

The cohesive energies and configuration energy per atom were also computed for the different wall thickness of HQDs with 3nm radius and presented in Fig.3a. The corresponding heat capacity per atom in Ev/K unit is also shown in Fig.3b.

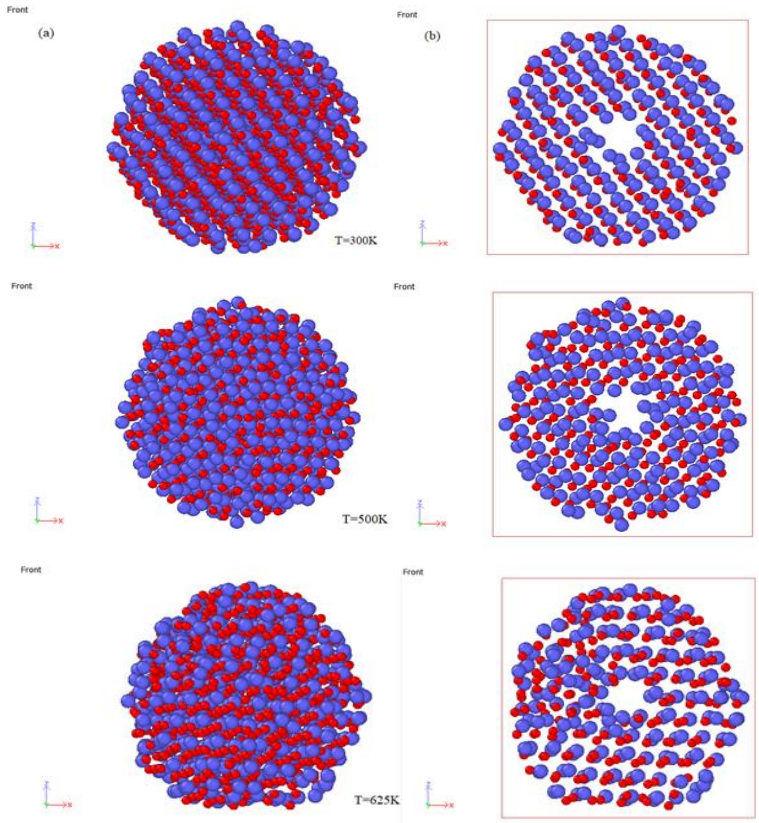

Fig. 2. Snapshots of front view for cross-sections of the CdSe (a)HQDs with N1190 atoms (b)sliced HQDs in [010] direction. Coloring denotes type of atom: blue for Cd, and red for Se

As it is evident from Fig.2 that both Cd and Se atoms fill the hollow interior during the heating process. Therefore, at 650K, the hollow region is quickly filled and suddenly collapsed. Thus, thermodynamic stability occurs at the melting point of the inner part with the cohesive energy of the system tends to the minimum value. This stability can be observed in Fig.1. for the HQDs with the t=1.5nm wall thickness.

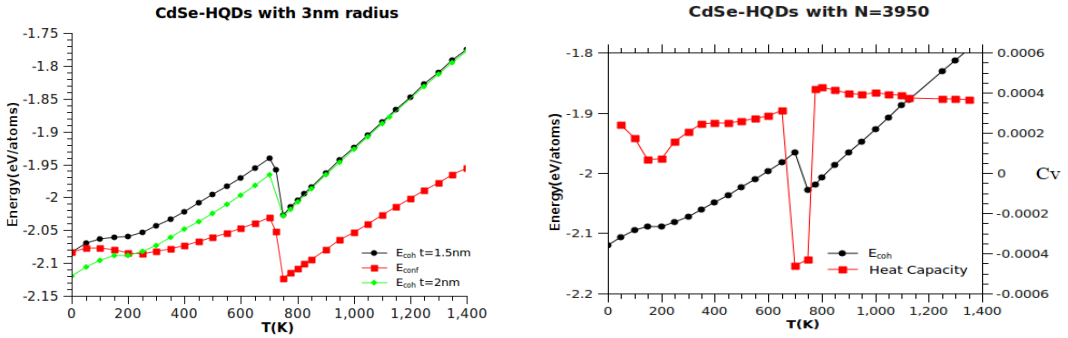

a) b)

Fig.3: Temperature dependence of (a) calculated Energies and (b)the corresponding isochoric heat capacity of CdSe HQDs with 3nm radius

As shown in Fig.3, by increasing the wall thickness, resulting in lower cohesive energies and heat capacity. It can be seen in Fig.3a that the configurational energy of HQDs is lower than those of cohesive energies. An abrupt rise/drop in the potential energy curve appears at the temperature around 650K after the continuously linear increase, corresponding to a sharp decrease in the heat capacity curve. The temperature corresponds to the maximum of the peak in heat capacity is defined as the melting temperature. The minimum value of the heat capacity corresponds to the temperature for which a sharp decrease in the cohesive energy curves can be observed in Fig.3b. That temperature indicates the phase transition in inner part of HQDs.

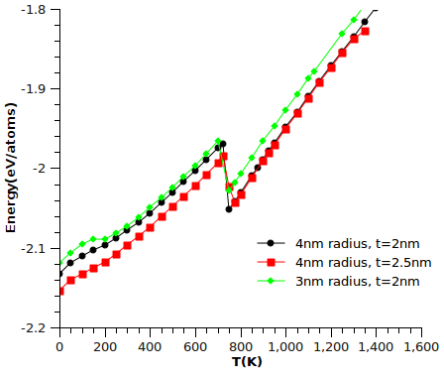

Fig. 4. Temperature dependence of the cohesive energy of HQDs with 4nm radius in comparison with 3nm radius at the same thickness

On the based of the results given in Figs.1, 3 and 4, it was found that the 4nm radius HQDs with the least cohesive energy has the highest thermodynamic stability. It seems in Fig.4 that the abrupt change in cohesive energy characterized by the first step melting of the hollow inner shell. It is noticeable that for the minor change in the energy curve, due to the small positive jump in the heat capacity, the second stage melting (solid-liquid transition) can be observed in atomic diffusion kinetics as the whole melting of HQDs. The atomic diffusions in different sizes of HQDs are given in Fig. 5.

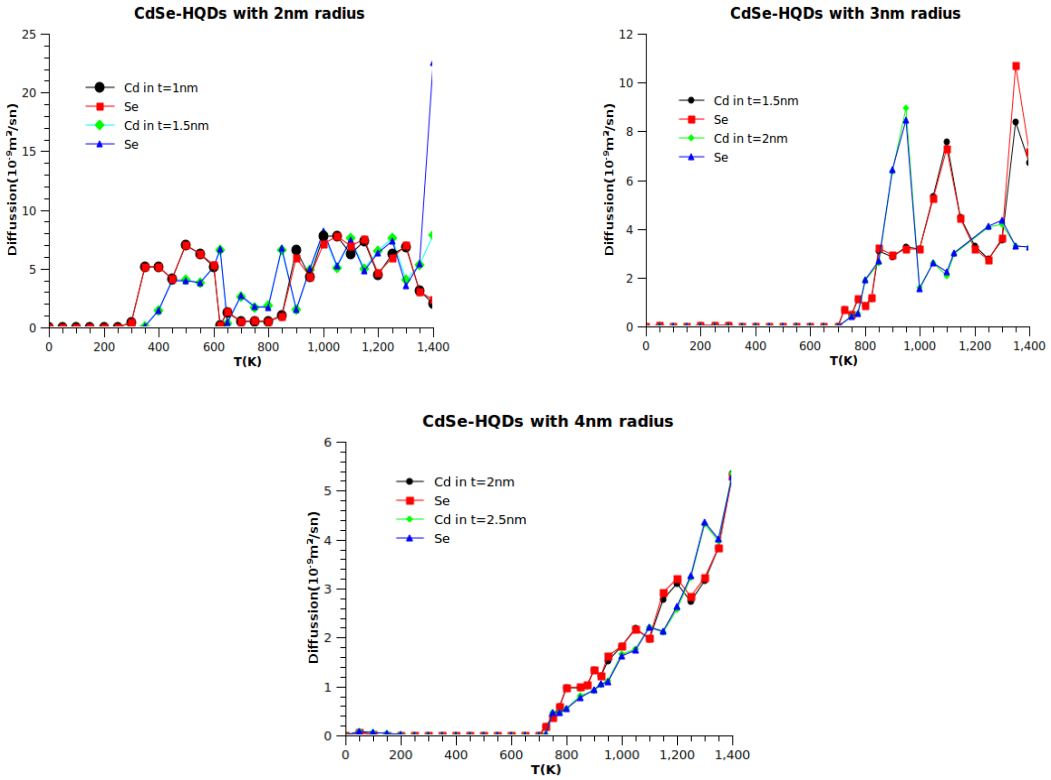

Fig.5. Self-Diffusion coefficients of Cd and Se atoms in different size of HQDs under heating.

Evidently, a typical two-stage melting (the first stage is rapid but second stage is slow) in these last two QDs can be verified from Fig.5, consistent with the results of cohesive energy and heat capacity given in Figs.3-4.

4. Conclusions

The main purpose of this work was to investigate the thermal properties of CdSe-HQDs by MD simulations. By analyzing the simulation results with caloric curves, heat capacities, and diffusion coefficients, the thermally induced two-step phase transformations in the simulated CdSe-HQDs were also determined for the HQDs with diameters larger than 5nm. The first order phase transition can be identified clearly for 6nm and partially for 8nm size CdSe-HQDs.

References

[1] M. Green, Semiconductor Quantum Dots: Organometallic and Inorganic, RSC Nanoscience and Nanotechnology **33**, 1 (2014).
[2] A. Qurashi: Metal Chalcogenide Nanostructures for Renewable Energy Applications, Wiley, New York, (2015).
[3] D. Bera, L. Qian, Semiconducting Quantum Dots for Bioimaging, Information Healthcare, New York, U.S. 191 (2009).
[4] A. A. Chistyakov, M. A. Zvaigzne,V. R. Nikitenko, A. R. Tameev, I. L. Martynov, O. V. Prezhdo, J Phys. Chem. Lett. **8**, 4129 (2017).
[5] K. B. Subila, G. K. Kumar, S. M. Shivaprasad and G. K. Thomas, J Phys. Chem. Lett. **4**, 2774 (2013).
[6] T. Xuan, X. Wang, G. Zhu, H. Li, L. Pan, Z. Sun, J. Alloys and Comp. **558**, 105 (2013).

[7] A. Bansal, S. S. Verma, Plasmonics **9**, 335 (2013).
[8] S. Gullapalli1, J. M. Grider, H. G. Bagaria, K.-S Lee, M. Cho, V. L Colvin, G. E. Jabbour M. S. Wong, Nanotechnology **23**, 495605 (2012).
[9] A. Gadall, M. S. Abdel-Sadek, R. Hamood, Chal. Letters **14**(7), 239 (2017).
[10] H. I. Ikeri, A. I. Onyia, P. U. Asogwa, Chal. Letters, **14**(2), 49 (2017).
[11] Y. Chen, D. Chen, Z.Li, X. Peng, J. Am. Chem. Soc. **139**, 10009 (2017).
[12] J. W. Kim, H-S Shim, J. G. Lee and W. B. Kim, J. Mater. Sci. **49**, 2912 (2014).
[13] Y. Wang, B. Zou, G. Li and S. Zhou, Materials Letters **65**, 1601 (2011).
[14] L. Guo, S. Zhang, W. Feng, G. Hu and W. Li, J. Alloys, and Comp. **579**,583 (2013).
[15] S. Ouendadji, S. Ghemid, H. Meradji, F. El Haj Hassan, Comput. Mater. Sci. **50**, 1460 (2011).
[16] Z. Fan, A.O. Yalcin, F. D. Tichelaar, H.W. Zandbergen,E.Talgorn,A.J. Houtepen, T. J. H. Vlugt,M. A. van Huis, J. Am. Chem. Soc. **135**, 5869 (2013).
[17] J. Tersoff, Phys. Rev. B. **39**, 5566 (1989).
[18] F. Benkabou, H. Aourag and M. Certier, Mater. Chem. Phys. **66**, 10 (2000).
[19] DL_POLY: a molecular dynamics simulation package was written by W. Smith, T.R. Forester, I.T. Todorov obtained from the website http://www.ccp5.ac.uk/DL_POLY
[20] S. Stelmakh, K. Skrobas, S. Gierlotka and B. Palosz, J. Nanopart Res. **19**, 170 (2017).
[21] S. Senturk Dalgic, published in Mater. Sci. Forum (2018).
[22] OVITO: A. Stukowski, Modelling Simul. Mater. Sci. Eng. 18 (2010), p. 015012.